

Alysson R. Carvalho
Peter M. Spieth
Paolo Pelosi
Marcos F. Vidal Melo
Thea Koch
Frederico C. Jandre
Antonio Giannella-Neto
Marcelo Gama de Abreu

Ability of dynamic airway pressure curve profile and elastance for positive end-expiratory pressure titration

Received: 15 October 2007
Accepted: 8 September 2008
Published online: 30 September 2008
© Springer-Verlag 2008

Electronic supplementary material

The online version of this article (doi:[10.1007/s00134-008-1301-7](https://doi.org/10.1007/s00134-008-1301-7)) contains supplementary material, which is available to authorized users.

M. G. de Abreu (✉)
Pulmonary Engineering Group,
Department of Anesthesiology
and Intensive Care Therapy,
University Hospital Dresden,
Fetscherstrasse 74,
01307 Dresden, Germany
e-mail: mgabreu@uniklinikum-dresden.de
Tel.: +49-351-4582785
Fax: +49-351-4584336
URL: <http://tu-dresden.de/peg>

obtained at end-expiratory and end-inspiratory pauses. The elastance of the respiratory system (Ers), the stress index and the percentage of volume-dependent elastance (%E₂) were estimated. *Measurements and main results:* In non-injured and injured lungs, the PEEP at which Ers was lowest (8–4 and 16–12 cmH₂O, respectively) corresponded to the best compromise between recruitment/hyperinflation. In non-injured lungs, stress index and %E₂ correlated with tidal recruitment and hyperinflation. In injured lungs, stress index and %E₂ suggested overdistension at all PEEP levels, whereas the CT scans evidenced tidal recruitment and hyperinflation simultaneously. *Conclusion:* During ventilation with low tidal volumes, Ers seems to be useful for guiding PEEP titration in non-injured and injured lungs, while stress index and %E₂ are useful in non-injured lungs only. Our results suggest that Ers can be superior to the stress index and %E₂ to guide PEEP titration in focal loss of lung aeration.

Abstract Objective: To evaluate the ability of three indices derived from the airway pressure curve for titrating positive end-expiratory pressure (PEEP) to minimize mechanical stress while improving lung aeration assessed by computed tomography (CT). *Design:* Prospective, experimental study. *Setting:* University research facilities. *Subjects:* Twelve pigs. *Interventions:* Animals were anesthetized and mechanically ventilated with tidal volume of 7 ml kg⁻¹. In non-injured lungs (n = 6), PEEP was set at 16 cmH₂O and stepwise decreased until zero. Acute lung injury was then induced either with oleic acid (n = 6) or surfactant depletion (n = 6). A recruitment maneuver was performed, the PEEP set at 26 cmH₂O and decreased stepwise until zero. CT scans were

A. R. Carvalho · P. M. Spieth · T. Koch ·
M. G. de Abreu
Clinic of Anesthesiology and Intensive
Care Therapy, Medical Faculty,
University Hospital Carl Gustav Carus,
Dresden, Germany

A. R. Carvalho · F. C. Jandre ·
A. Giannella-Neto
Program of Biomedical Engineering,
COPPE, Federal University of
Rio de Janeiro, Rio de Janeiro, Brazil

P. Pelosi
Department of Ambient, Health and Safety,
University of Insubria, Varese, Italy

M. F. Vidal Melo
Department of Anesthesia and Critical Care,
Massachusetts General Hospital,
Harvard Medical School,
Boston, MA, USA

Keywords Acute lung injury ·
Lung protective strategy ·
Ventilator-induced lung injury

Introduction

Mechanical ventilation strategies aimed at avoiding tidal recruitment/overdistension seem to minimize ventilator-associated lung injury both in experimental and clinical acute lung injury (ALI) [1, 2]. In this context, the analysis of the shape of the dynamic airway pressure (P_{aw}) curve may allow detection of tidal recruitment/overdistension and, therefore, be useful for positive end-expiratory pressure (PEEP) titration [3–6].

When the inspiratory flow is constant, the concavity of the P_{aw} curve can be described by a dimensionless coefficient known as “stress index”. A stress index > 1.1 indicates tidal overdistension (upward concavity), whereas values < 0.9 indicate tidal recruitment (downward concavity). Accordingly, values of stress index ≈ 1 are associated with protective ventilation [1, 7, 8].

Another proposed index to detect tidal recruitment/overdistension is the so-called $\%E_2$, which represents the percentage of non-linearity of the elastance of the respiratory system (E_{rs}). It has been suggested that $\%E_2 < 0\%$ is associated with tidal recruitment, whereas $\%E_2 > 30\%$ is associated with tidal overdistension [4, 5].

Alternatively, the linear E_{rs} may be also useful to guide PEEP titration [9–11]. It was claimed that PEEP at which E_{rs} is minimal corresponds to a compromise between the distribution of aeration and mechanical stress [9, 10].

In the present study, we investigated the ability of the stress index, $\%E_2$ as well as E_{rs} for guiding PEEP titration during a decremental PEEP trial to minimize mechanical stress while improving lung aeration assessed by computed tomography (CT).

Materials and methods

The materials and methods are described in detail in the Electronic Supplementary Material (ESM) accompanying this article, and briefly summarized here.

Experimental protocols

Two protocols were performed in different institutions and approved by the respective local animal care Committees in Brazil and Germany. Twelve mixed-breed female Landrace/Large White pigs were used. In six of them, ALI was induced by oleic acid (oleic acid injury) in Brazil, whereas surfactant depletion (lavage injury) was used in other six animals in Germany. Animals were anesthetized and ventilated with $F_{I}O_2$ equal to 1.0, PEEP of 5 cmH_2O , inspiratory/expiratory ratio of 1:2 and tidal volume (V_T) of 7 ml/kg. Respiratory rates were adjusted to achieve a $PaCO_2$ between 35 and 45 mmHg at baseline and maintained unchanged thereafter.

After 15-min stabilization, baseline measurements were obtained. Before induction of injury with oleic acid (non-injury, $n = 6$), PEEP was sequentially set at 16, 12, 8, 6, 4 and 0 cmH_2O (5 min/level), while other settings were kept constant. Then, PEEP was set at 5 cmH_2O and ALI induced by central venous injection of oleic acid in aliquots of 0.05 ml kg^{-1} until $PaO_2/FiO_2 < 200$ mmHg (oleic acid injury, $n = 6$).

Lavage injury was induced by repetitive lung lavage with warmed saline (lavage injury, $n = 6$) [12] until $PaO_2/FiO_2 < 200$ mmHg. In both models, injury was considered stable if PaO_2/FiO_2 did not improve within 30 min.

Following injury, a recruitment maneuver was performed (40 cmH_2O constant P_{aw} , 30 s) and PEEP sequentially set at 26, 20, 16, 12, 8, 6 and 0 cmH_2O (5 min/level).

Assessment of linear respiratory system elastance and airway pressure curve profile analysis

P_{aw} and airway flow were recorded in a computer with a sample rate of 200 samples/s. Thereafter, the P_{aw} was fitted to:

1. A linear single-compartment model (Eq. 1), for the estimation of the E_{rs} [13];

$$P_{aw} = E_{rs} \cdot V + R_{rs} \cdot \dot{V} + EEP \quad (1)$$

where R_{rs} is the resistance of the respiratory system, \dot{V} is the airway flow, V is the volume and EEP is the end-expiratory pressure.

2. A volume-dependent single-compartment model (Eq. 2), which is an extension of the model presented in the Eq. 1, for the estimation of the $\%E_2$ (Eq. 3) [3, 4];

$$P_{aw} = (E_1 + E_2 \cdot V) \cdot V + R_{rs} \cdot \dot{V} + EEP \quad (2)$$

$$\%E_2 = 100 \cdot (E_2 \cdot V_T) / (E_1 + E_2 \cdot V_T) \quad (3)$$

where E_1 and $E_2 \cdot V$ are the volume-independent and dependent components of the E_{rs} , respectively.

3. An airway pressure–time model (Eq. 4), for the estimation of the stress index [4];

$$P_{aw} = a \cdot t_i^b + c \quad (4)$$

where a , b and c are constants, and t_i is the inspiratory time related to the constant part of the inspiratory flow. The coefficient b is known as stress index.

A stress index = 1.0 and $\%E_2 = 0$ indicate a straight P_{aw} curve profile. The PEEP at which the E_{rs} was

minimal, the stress index was close to 1 and % E_2 to 0% was considered the optimal PEEP. Statistical analysis

CT scan procedure and image analysis

Helical CT scans were obtained between the base of the heart and the right dome of the diaphragm. Images were reconstructed yielding five to seven slices of 1 mm thickness.

Static CT scans were obtained in both groups at each PEEP during end-expiratory and end-inspiratory breath holds (15–20 s). To achieve comparability of CT scans among PEEP levels, a new topogram was acquired at each PEEP and the juxta-diaphragmatic region selected. For analysis, we chose one slice at end-expiration and another one at end-inspiration showing the highest anatomical matching. After manual delineation of the lung parenchyma, the slice volume as well as the volumes of hyperinflated, normally-, poorly-, and non-aerated regions were calculated [14]. The fractions of recruitment and hyperinflation induced by PEEP, as well as of tidal recruitment and hyperinflation were calculated as described elsewhere [15–17].

Data are expressed as median and ranges. Association between the stress index, % E_2 and CT-scan evidences of tidal recruitment/hyperinflation were determined by linear regression. The Wilcoxon signed rank test was used to compare changes in variables investigated at each level of PEEP. The Bonferroni–Holm procedure was used for the adjustment of multiple comparisons. A $P < 0.05$ was considered statistically significant in all tests.

Results

The induction of ALI impaired oxygenation and increased Ers ($P < 0.05$, Table ESM-1 and Table ESM-2).

Non-injury

Table 1 shows the data for non-injured lungs. The reduction of PEEP decreased the amount of hyperinflated

Table 1 Lung mechanics and aeration distribution in non-injury

PEEP (cmH ₂ O)	Decremental trial					
	16	12	8	6	4	0
P_{peak} (cmH ₂ O)	28 (24–31)	20 (19–22)*	15 (14–18)*	12 (11–14)*	11 (10–12)*	8 (7–10)*
P_{plat} (cmH ₂ O)	25 (22–28)	18 (17–19)*	14 (12–15)*	11 (10–12)*	9 (8–10)*	6 (6–7)*
Ers (cmH ₂ O l ⁻¹)	55 (42–72)	34 (30–37)*	30 (26–39)*	29 (25–35)	30 (27–32)	36 (30–43)*
Stress index	1.2 (1.1–1.2)	1.0 (1.0–1.1)*	0.9 (0.9–1.0)*	0.8 (0.8–0.9)	0.8 (0.8–0.8)	0.7 (0.6–0.8)*
% E_2	21 (15–37)	4 (2–5)*	–6 (–13–3)*	–11 (–14 to –5)	–14 (–18–10)*	–26 (–31 to –21)*
Hyperinflated (%slice volume)						
End-expiration	53 (24–60)	42 (16–46)*	22 (9–28)*	17 (6–17)*	11 (3–15)*	6 (1–7)*
End-inspiration	62 (46–72)	49 (28–62)*	34 (15–38)*	27 (10–31)*	19 (8–21)*	13 (4–17)*
Tidal hyperinflation (%)	35 (32–44)	26 (14–38)*	19 (8–21)*	15 (4–16)*	9 (7–13)*	9 (4–15)*
Normally (%slice volume)						
End-expiration	50 (33–68)	61 (46–74)*	69 (64–77)*	74 (71–78)*	78 (74–79)	79 (71–80)
End-inspiration	28 (21–47)	36 (31–63)*	55 (53–75)*	66 (60–79)*	71 (69–77)*	77 (70–77)*
Poorly-aerated (%slice volume)						
End-expiration	6 (5–7)	7 (6–8)	7 (6–10)	9 (7–12)*	10 (8–16)*	16 (11–23)*
End-inspiration	6 (5–8)	6 (5–8)	7 (6–8)	8 (7–9)	9 (7–12)	10 (8–15)*
Non-aerated (%slice volume)						
End-expiration	2 (2–2)	2 (2–3)	2 (2–3)	3 (2–3)	3 (2–4)	4 (2–4)*
End-inspiration	2 (2–2)	2 (2–2)	2 (2–3)	2 (2–3)	3 (2–3)	3 (2–4)
Tidal recruitment (%)	0 (0–1)	0 (0–2)	0 (0–3)	0 (0–3)	1 (1–4)*	4 (3–9)*

Data are presented as median range values

PEEP Applied positive end-expiratory pressure; P_{peak} , peak ventilator pressure; P_{plat} , plateau ventilator pressure; Ers, elastance of the respiratory system; stress index, overdistension index from the airway pressure-time model; % E_2 , overdistension index from the volume dependent single compartmental model; Hyperinflated (%slice volume), percentage of the hyperinflated lung regions related to slice volume; Normally (%slice volume), percentage of the normally aerated lung regions related to slice volume; Poorly-aerated (%slice volume), percentage of the poorly aerated lung regions related to slice volume; Non-aerated (%Slice volume),

percentage of the non-aerated lung regions related to slice volume; Tidal hyperinflation, fraction of change of hyperinflated regions from expiration to inspiration related to the volume of normally aerated regions at expiration; Tidal recruitment, fraction of change of poorly and non-aerated areas from expiration to inspiration related to the volume of normally aerated regions at expiration; End-expiration, values obtained with an end-expiratory pause; End-Inspiration, values obtained with an end-inspiratory pause

* $P < 0.05$ versus the immediately precedent value (Wilcoxon sign rank test)

areas and increased normally aerated ones ($P < 0.05$). PEEP < 12 cmH₂O increased poorly aerated areas, while non-aerated ones increased at PEEP < 4 cmH₂O ($P < 0.05$).

The Ers exhibited a flat minimum from PEEP of 8–4 cmH₂O. In this range a balance between the maximization of normally aerated regions and the minimization of non-, poorly-, and hyper-aerated regions was observed (Table 1).

Reduction of PEEP progressively decreased tidal hyperinflation and reduced stress index and %E₂. At PEEP levels ranging from 12 to 8 cmH₂O, the stress index and %E₂ were not associated with cyclic collapse/reopening or overdistension. At PEEP levels < 8 cmH₂O, the stress index was < 0.9 , %E₂ $< 0\%$ and tidal recruitment increased ($P < 0.05$). As shown in Fig. 1, the stress index and %E₂ correlated with tidal hyperinflation ($r^2 = 0.69$, $P = 0.0001$) and tidal recruitment ($r^2 = 0.35$, $P = 0.0001$).

Figure 2 (left) shows CT-scan images (Panel A), Ers (Panel B), stress index (Panel C), %E₂ (Panel D), fractions of hyperinflation and recruitment (Panel E), tidal hyperinflation and recruitment (Panel F) at each PEEP in all non-injured lungs. A focal pattern of loss of aeration was observed at PEEP ≤ 4 cmH₂O, whereas a balance between hyperinflation and recruitment occurred at PEEP

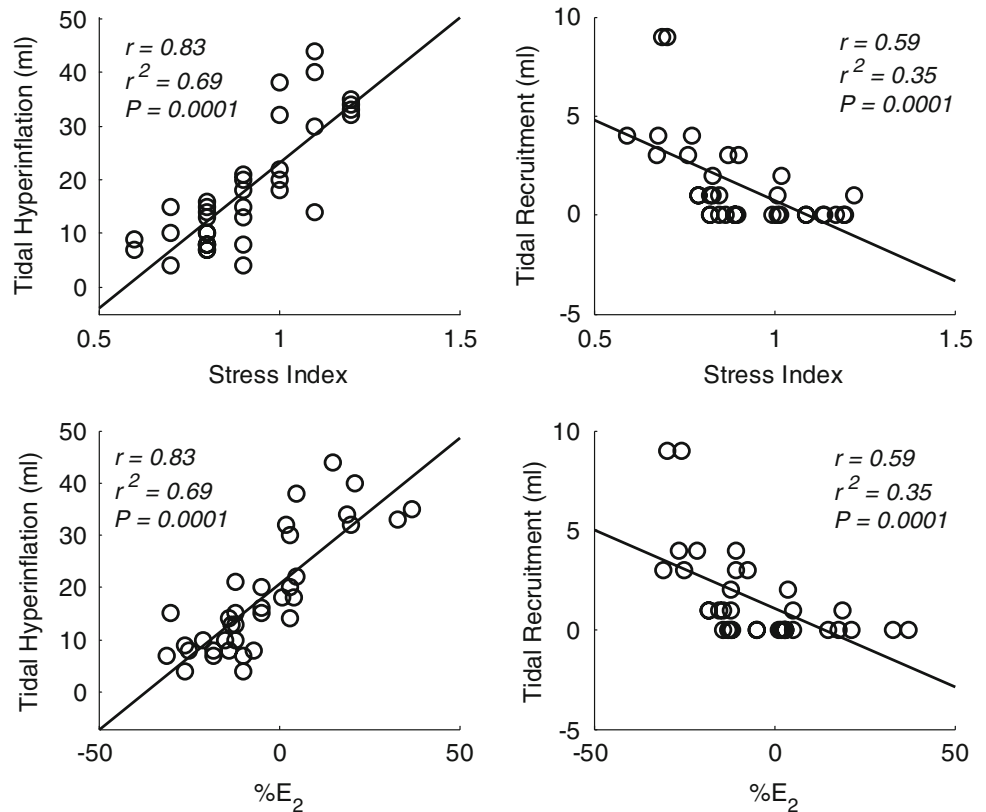
of 12 and 8 cmH₂O. Tidal hyperinflation was predominant in non-dependent lung regions.

Oleic acid and lavage injury

Tables 2 and 3 show data for oleic acid and lavage injury, respectively. Reduction of PEEP progressively decreased hyperinflated and normally aerated areas, while increasing poorly and non-aerated ones. Ers showed a flat minimum from the PEEP of 16–12 cmH₂O and from 12 to 8 cmH₂O, in oleic acid and lavage injury, respectively. PEEP lower than the PEEP at which Ers was minimal resulted in a significant increase of poorly and non-aerated areas, and decrease of normally aerated areas (Tables 2, 3). Oleic acid injury showed less normally aerated areas at PEEP < 6 cmH₂O and less hyperinflated areas at PEEP > 20 cmH₂O, when compared to lavage injury ($P < 0.05$).

The stress index and %E₂ achieved values higher than 1.0 and 0%, respectively, in almost all PEEP levels, independently of the ALI model. No significant changes in stress index and %E₂ could be detected when PEEP was reduced. In lavage injury, %E₂ was higher compared to oleic acid injury ($P < 0.05$). Higher amounts of hyperinflated areas were also observed in lavage injury (Tables 2, 3). In lavage injury, stress index and %E₂ were

Fig. 1 Relationship between values of stress index and %E₂ and amount of tidal hyperinflation (left column) and tidal recruitment (right column) measured at all levels of positive end-expiratory pressure (PEEP) in non-injured animals



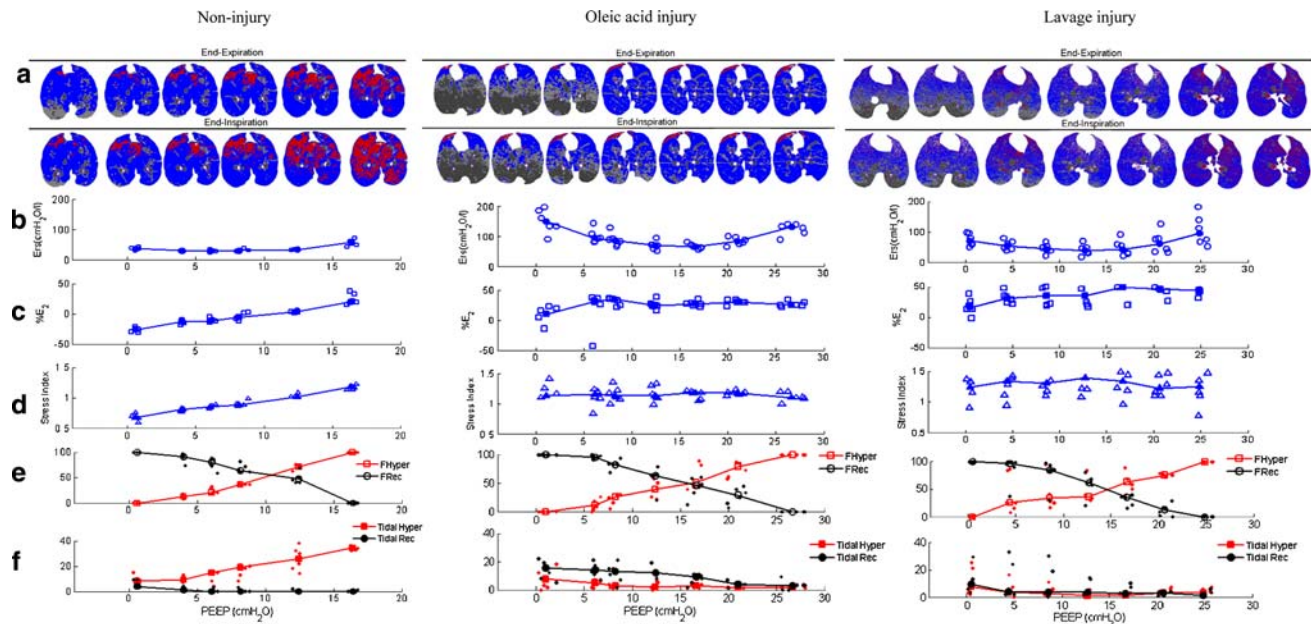


Fig. 2 Distribution of aeration as a function of PEEP in non-injured (*left panels*), oleic acid (*midpanels*) and lavage (*right panels*) injured animals. **a** Regions of interest in the CT scan images obtained in a representative animal at each PEEP level: *red* hyperinflation, *blue* normal aeration, *light gray* poor aeration, *dark gray* non-aeration. Note the focal loss of aeration in dependent lung regions at lower PEEP and the hyperinflation of non-dependent regions throughout inspiration; **b–d** elastance of the respiratory system, $\%E_2$ and stress index. *Open and filled symbols* represent

individual and median values, respectively; **e** median fractions of hyperinflation (FHyp, *open red squares*) and recruitment (FRec, *open black circles*) at end-expiration, i.e., induced by PEEP. *Red and black dots* represent individual values of fractional hyperinflation and recruitment, respectively; **f** median tidal hyperinflation (Tidal Hyper, *filled red squares*) and recruitment (Tidal Rec, *filled black circles*) (ml). *Red and black dots* represent individual values of hyperinflation and recruitment, respectively

inversely correlated with tidal hyperinflation ($r^2 = 0.1$ with $P = 0.05$, and $r^2 = 0.23$, $P = 0.001$, respectively). No correlation was observed between stress index and tidal recruitment ($r^2 = 0.008$, $P = 0.6$), but the $\%E_2$ was significantly correlated with tidal recruitment in the lavage model ($r^2 = 0.26$, $P = 0.0006$). In oleic acid injury, stress index and $\%E_2$ were inversely correlated only with tidal recruitment ($r^2 = 0.41$, $P < 0.0001$ and $r^2 = 0.73$, $P < 0.0001$, respectively).

Figure 2 shows CT-scan images (Panel A), Ers (Panel B), stress index (Panel C), $\%E_2$ (Panel D), the fraction of hyperinflation and recruitment (Panel E), tidal hyperinflation and recruitment (Panel F) at each PEEP in all studied animals with oleic acid and lavage injury (middle and left, respectively). A focal pattern of loss of aeration was observed in both ALI groups. PEEP led to recruitment in dependent regions and hyperinflation in non-dependent ones, simultaneously. Tidal recruitment/hyperinflation occurred simultaneously at all levels of PEEP in both ALI models. In oleic acid injury, tidal recruitment was higher, especially at PEEP lower than 20 cmH₂O.

In the ESM, dynamic CT movies in representative animals show the simultaneous occurrence of tidal

recruitment and hyperinflation in the same lungs at different PEEP levels. Stress index and $\%E_2$ indicated only overdistension in all situations.

Stress index versus $\%E_2$

The degree of correlation between the stress index and $\%E_2$ was $r = 0.93$ ($r^2 = 0.87$, $P < 0.0001$) for non-injured lungs, $r = 0.76$ ($r^2 = 0.58$, $P < 0.0001$) for oleic acid injury and $r = 0.36$ ($r^2 = 0.13$, $P = 0.018$) for lavage injury. The previously proposed threshold $\%E_2 > 30\%$ for overdistension [4, 5] did not match with stress index > 1.1 and CT-scan measurements of hyperinflation. Values of stress index ranging from 0.9 to 1.1 corresponded to $\%E_2$ in the range of -10 to 10% (Figure ESM 4).

Discussion

The main findings of the present study were that during low V_T strategy: (1) in non-injured lungs, PEEP > 12 cmH₂O

Table 2 Lung mechanics and aeration distribution in oleic acid injury

PEEP (cmH ₂ O)	Decremental trial						
	26	20	16	12	8	6	0
P_{peak} (cmH ₂ O)	47 (40–52)	36 (31–40)*	29 (26–31)*	25 (23–28)*	24 (21–26)*	24 (21–26)	24 (22–29)
P_{plat} (cmH ₂ O)	39 (34–46)	31 (29–37)*	26 (24–28)*	21 (19–25)*	19 (17–22)*	18 (16–22)*	18 (14–21)
Ers (cmH ₂ O l ⁻¹)	131 (90–141)	84 (65–101)*	65 (55–81)*	70 (53–96)	86 (67–129)*	94 (81–144)*	149 (91–198)*
Stress index	1.1 (1.0–1.2)	1.2 (1.1–1.2)	1.2 (1.0–1.3)	1.1 (1.0–1.3)	1.2 (1.0–1.4)	1.2 (1.1–1.7)	1.2 (0.4–1.4)
% E_2	23 (12–34)	24 (15–34)	23 (6–29)	18 (2–32)	31 (8–35)	33 (14–38)	8 (–13–24)
Hyperinflated (%slice volume)							
End-expiration	7 (2–15)	6 (1–11)	5 (1–8)	4 (1–5)	2 (0–7)	2 (0–4)*	1 (0–1)
End-inspiration	10 (4–18)	7 (3–14)*	6 (2–10)	4 (2–9)	4 (1–8)	3 (1–6)	2 (0–6)
Tidal hyperinflation (%)	3 (1–4)	1 (1–4)	3 (1–4)	2 (0–6)	3 (1–8)	5 (2–8)	8 (0–18)
Normally (%slice volume)							
End-expiration	73 (70–80)	72 (67–80)*	68 (63–80)*	56 (51–72)*	50 (34–61)*	47 (28–51)*	22 (12–46)*
End-inspiration	76 (69–79)	75 (70–80)	72 (70–81)	62 (56–78)*	54 (46–69)*	49 (35–63)*	34 (24–47)*
Poorly-aerated (%slice volume)							
End-expiration	15 (11–21)	15 (13–24)*	23 (15–31)*	31 (23–38)*	30 (17–37)	28 (23–37)	26 (24–41)
End-inspiration	13 (8–17)	14 (10–18)*	16 (13–23)	24 (17–30)*	24 (16–31)	24 (14–31)	25 (20–38)
Non-aerated (%slice volume)							
End-expiration	2 (1–4)	2 (2–4)	3 (2–6)	7 (3–12)*	18 (8–29)*	27 (12–41)*	47 (27–59)*
End-inspiration	2 (1–4)	2 (1–6)	3 (2–6)	6 (3–19)*	18 (6–23)*	24 (11–35)*	33 (26–51)*
Tidal recruitment (%)	3 (0–9)	4 (0–7)	9 (2–11)*	12 (8–20)*	13 (2–20)	14 (7–21)	10 (0–68)

Data are presented as median range values

PEEP Applied positive end-expiratory pressure; P_{peak} , peak ventilator pressure; P_{plat} , plateau ventilator pressure; Ers, elastance of the respiratory system; stress index, overdistension index from the airway pressure-time model; % E_2 , overdistension index from the volume dependent single compartmental model; Hyperinflated (%slice volume), percentage of the hyperinflated lung regions related to slice volume; Normally (%slice volume), percentage of the normally aerated lung regions related to slice volume; Poorly-aerated (%slice volume), percentage of the poorly aerated lung regions related to slice volume; Non-aerated (%slice volume),

percentage of the non-aerated lung regions related to slice volume; Tidal hyperinflation, fraction of change of hyperinflated regions from expiration to inspiration related to the volume of normally aerated regions at expiration; Tidal recruitment, fraction of change of poorly and non-aerated areas from expiration to inspiration related to the volume of normally aerated regions at expiration; End-expiration, values obtained with an end-expiratory pause; End-inspiration, values obtained with an end-inspiratory pause
* $P < 0.05$ versus the immediately precedent value (Wilcoxon sign rank test)

induced hyperinflation at end-expiration and during tidal breathing (tidal hyperinflation), and increased Ers, stress index and % E_2 ; (2) in injured lungs, PEEP simultaneously recruited dependent lung regions and hyperinflated non-dependent ones, but stress index and % E_2 suggested tidal overdistension; (3) PEEP at which Ers was minimal always resulted in the best compromise between recruitment and hyperinflation.

Non-injured lungs

Significant amounts of hyperinflation and tidal hyperinflation in non-dependent lung regions were observed at PEEP > 8 cmH₂O. In agreement with our previous works [9], the hyperinflation induced by PEEP was associated with an increase in Ers. When animals were ventilated with PEEP < 6 cmH₂O, the increase of poorly aerated areas was also associated with an increase of Ers. Interestingly, tidal recruitment of dependent regions occurred simultaneously with some degrees of tidal hyperinflation of non-dependent regions.

Despite the complex aeration patterns, both stress index and % E_2 indicated cyclic collapse/re-opening. This

confirms previous observations that, in non-injured lungs, tidal recruitment is associated with cyclic closure/re-opening of airways [18, 19], particularly at low PEEP [19]. Furthermore, the stress index and % E_2 correlated well with tidal hyperinflation.

The PEEP at which Ers was minimal corresponded to the best compromise between recruitment and hyperinflation [9], and was close to the PEEP at which the stress index and % E_2 indicated a straight Paw curve.

Hyperinflation and tidal hyperinflation occurred even at zero PEEP, explained by an increase in alveolar air content and/or reduction in regional perfusion, and/or changes in regional transpulmonary pressure gradient, favoring the increase of aeration in non-dependent lung zones [20].

Thus, our results suggest that Ers, stress index and % E_2 could be useful to guide PEEP titration in non-injured lungs, for example during general anesthesia.

Acute lung injury

At low PEEP levels, a focal loss of aeration was observed in dependent lung regions in both ALI models. However, compared to oleic acid injury, lavage injury showed

Table 3 Lung mechanics and aeration distribution in lavage injury

PEEP (cmH ₂ O)	Decremental trial						
	26	20	16	12	8	6	0
P_{peak} (cmH ₂ O)	49 (42–61)	35 (31–45)*	28 (24–34)*	24 (21–26)*	21 (19–22)	19 (17–21)	19 (16–23)
P_{plat} (cmH ₂ O)	39 (30–52)	27 (21–40)*	23 (20–29)*	19 (13–22)*	15 (10–28)*	15 (13–16)	13 (11–17)
Ers (cmH ₂ O l ⁻¹)	94 (53–181)	60 (33–127)*	43 (21–92) [#]	40 (18–70)	45 (22–68)*	54 (39–80)*	70 (50–97)*
Stress index	1.2 (0.8–1.5)	1.2 (1.1–1.5)	1.3 (1.0–1.7)	1.4 (1.1–1.8)	1.3(1.1–1.7)	1.3 (1.0–1.9)	1.2 (0.4–1.5)
% E_2	44 (31–54)	46 (26–53)	49 (20–56)	36 (17–57)	35 (19–50)	30 (21–47)	16 (–2–38)
Hyperinflated (%slice volume)							
End-expiration	13 (9–15)	12 (8–14)	9 (8–14)	8 (5–14)	9 (3–12)	7 (2–12)	5 (1–7)
End-inspiration	16 (10–20)	14 (9–17)	11 (9–15)	9 (8–15)	10 (8–13)	9 (7–13)	8 (6–12)
Tidal hyperinflation (%)	3 (1–7)	3 (1–7)	2 (0–3)	1 (0–5)	3 (1–11)	4 (0–16)	8 (2–25)
Normally (%slice volume)							
End-expiration	76 (70–78)	74 (60–77)	71 (58–76)	63 (54–73)*	53 (44–62)*	51 (36–57)	46 (28–52)
End-inspiration	73 (62–78)	72 (61–80)	73 (55–75)	68 (55–75)	58 (52–64)*	53 (50–58)*	50 (41–52)
Poorly-aerated (%slice volume)							
End-expiration	8 (5–13)	13 (6–20)	15 (9–22)	18 (9–31)*	23 (16–36)*	25 (17–35)*	33 (19–38)*
End-inspiration	6 (2–15)	8 (2–17)	10 (4–20)	15 (4–23)*	21 (14–23)*	23 (18–25)*	24 (18–26)*
Non-aerated (%slice volume)							
End-expiration	3 (1–6)	3 (1–6)	5 (3–6)	5 (3–9)	14 (6–16)*	16 (9–25)*	26 (17–31)*
End-inspiration	2 (0–6)	2 (1–6)	4 (2–6)	4 (3–9)	12 (4–16)*	16 (9–19)*	21 (13–29)*
Tidal recruitment (%)	2 (0–6)	3 (1–4)	3 (1–10)	4 (2–14)	4 (0–30)	4 (2–33)	10 (3–40)*

Data are presented as median range values

PEEP Applied positive end-expiratory pressure; P_{peak} , peak ventilator pressure; P_{plat} , plateau ventilator pressure; Ers, elastance of the respiratory system; stress index, overdistension index from the airway pressure-time model; % E_2 , overdistension index from the volume dependent single compartmental model; Hyperinflated (%slice volume), percentage of the hyperinflated lung regions related to slice volume; Normally (%slice volume), percentage of the normally aerated lung regions related to slice volume; Poorly-aerated (%slice volume), percentage of the poorly aerated lung regions related to slice volume; Non-aerated (%slice volume),

percentage of the non-aerated lung regions related to slice volume; Tidal hyperinflation, fraction of change of hyperinflated regions from expiration to inspiration related to the volume of normally aerated regions at expiration; Tidal recruitment, fraction of change of poorly and non-aerated areas from expiration to inspiration related to the volume of normally aerated regions at expiration; End-expiration, values obtained with an end-expiratory pause; End-inspiration, values obtained with an end-inspiratory pause
* $P < 0.05$ versus the immediately precedent value (Wilcoxon sign rank test)

higher amounts of normally aerated areas, favoring higher amounts of hyperinflated areas at high PEEP.

The association between the amount of normally aerated areas at zero PEEP and the potential of hyperinflation of these areas when PEEP is applied has been previously described in patients with ALI/ARDS presenting with a focal pattern of loss of aeration [21]. In both ALI models PEEP induced recruitment of poorly and non-aerated areas simultaneously to hyperinflation of previously aerated regions as also reported in human ALI/ARDS [14, 22, 23].

Similar to non-injured lungs, the PEEP at which Ers was minimal corresponded to the best compromise between recruitment and hyperinflation. In agreement with previous findings [9–11], high PEEP increased hyperinflation, whereas low PEEP increased poorly and non-aerated areas and reduced the amount of normally aerated areas.

The CT analysis showed a complex aeration pattern in both ALI models, with tidal recruitment and hyperinflation occurring simultaneously. Interestingly, both tidal recruitment and tidal hyperinflation increased as PEEP was reduced. In lavage injury they occurred almost in the same proportion, whereas in oleic acid injury tidal recruitment outweighed tidal hyperinflation. Since oleic acid injury presented less amounts of normally aerated

areas compared to lavage injury, it is possible that more recruitment occurred during inspiration.

The finding that in injured lungs the stress index was uniformly higher than 1.0 and % E_2 higher than 0%, irrespective of PEEP level, is striking. Indices derived from the Paw curve reflect global Ers variation through inspiration. Since both ALI models showed a focal loss of aeration at low PEEP, hyperinflation of the more compliant non-dependent regions and recruitment of dependent regions occurred simultaneously. Furthermore, tidal hyperinflation seems to be associated with alveolar overdistension [21, 24, 25], resulting in progressive Ers increase [9, 10]. On the other hand, a similar increase in Ers can be expected during tidal recruitment of previously poorly and non-aerated areas.

By increasing PEEP, an almost linear increase in hyperinflation occurred and was associated with an almost linear decrease in poorly/non-aerated tissue. Similarly, increase of PEEP led to a progressive decrease in tidal recruitment and hyperinflation. Thus, we were unable to find a level of PEEP at which the recruitment was maximized and no hyperinflation occurred.

Our findings partially differ from those by Grasso et al. [26], who suggested that stress index is able to detect tidal recruitment/hyperinflation in experimental

ALI. The most likely explanation is that we used low V_T (7 ml kg^{-1}), whereas Grasso et al. worked with high V_T (12 to 18 ml kg^{-1}). When high V_T is used, a clear predominance of tidal recruitment, at low levels of PEEP, or hyperinflation, at high levels of PEEP, is possible. Our findings are supported by Terragni et al. [27], who proposed that simultaneous recruitment and hyperinflation may explain the relatively low specificity of the concavity of the Paw curve in detecting VILI. In addition, we computed tidal recruitment considering the tidal variation of poorly and non-aerated areas, whereas Grasso et al. [26] considered only the variations of non-aerated areas. It is possible that higher amount of hyperinflation than recruitment occurs when a recruitment maneuver is not performed [28]. However, as shown in Tables 2 and 3 the exclusion of poorly aerated areas computation would not change our overall main findings.

Limitations

First, the use of different experimental facilities could have influenced our results. However, measurements followed standard international procedures and were consistent among different ALI models, using identical CT-scan configurations as well as mechanical ventilation settings. Second, similar to others [26] we used only one juxta-diaphragmatic CT slice, making it difficult to compare the same areas at different pressures. However, we selected images with maximal anatomical-landmarks coincidence, and a new topogram was acquired at each step. Third, the thresholds for CT compartments we used likely resulted in underestimation of hyperinflation in ALI, but

they correspond to those ones internationally recommended [21, 29–32]. Fourth, since measurements were taken during breath hold, it is possible that a redistribution of aeration occurred (pendelluft), but its effect on our measurements are likely negligible [33]. Fifth, it could be argued that time intervals of 5 min at each PEEP level were not enough to allow stable measurements. However, recruitment and derecruitment become stable as fast as 4 s in both the oleic acid and surfactant depletion models of ALI [34]. Based on this, we believe that complete stabilization of lung compartments should have occurred at the end of each PEEP step. Sixth, our results apply only for ALI with focal loss of aeration. Thus, we cannot exclude that stress index and $\%E_2$ may be useful to guide PEEP titration in presence of diffuse loss of lung aeration.

Conclusions

The PEEP at which Ers was minimal corresponded to the best compromise between recruitment/overdistension in non-injured and injured lungs. Stress index and $\%E_2$ were able to identify tidal recruitment/overdistension only in non-injured lungs. Our results suggest that Ers can be superior to the stress index and $\%E_2$ to guide PEEP titration in presence of focal loss of lung aeration.

Acknowledgments This work was supported by grants from the Brazilian Agencies CNPq and FAPERJ, the Clinic of Anesthesiology of the University Hospital Carl Gustav Carus, Technical University Dresden, Germany and by grant no. HL-086827 from the National Institutes of Health, Bethesda, MA, USA.

References

- Ranieri VM, Zhang H, Mascia L, Aubin M, Lin CY, Mullen JB, Grasso S, Binnie M, Volgyesi GA, Eng P, Slutsky AS (2000) Pressure-time curve predicts minimally injurious ventilatory strategy in an isolated rat lung model. *Anesthesiology* 93:1320–1328
- Grasso S, Stripoli T, De MM, Bruno F, Moschetta M, Angelelli G, Munno I, Ruggiero V, Anaclerio R, Cafarelli A, Driessen B, Fiore T (2007) ARDSnet ventilatory protocol and alveolar hyperinflation: role of positive end-expiratory pressure. *Am J Respir Crit Care Med* 176:761–767
- Ranieri VM, Giuliani R, Fiore T, Dambrosio M, Milic-Emili J (1994) Volume-pressure curve of the respiratory system predicts effects of PEEP in ARDS: “Occlusion” versus “Constant flow” technique. *Am J Respir Crit Care Med* 149:19–27
- Kano S, Lanteri CJ, Duncan AW, Sly PD (1994) Influence of nonlinearities on estimates of respiratory mechanics using multilinear regression analysis. *J Appl Physiol* 77:1185–1197
- Bersten AD (1998) Measurement of overinflation by multiple linear regression analysis in patients with acute lung injury. *Eur Respir J* 12:526–532
- Edibam C, Rutten AJ, Collins DV, Bersten AD (2003) Effect of inspiratory flow pattern and inspiratory to expiratory ratio on nonlinear elastic behavior in patients with acute lung injury. *Am J Respir Crit Care Med* 167:702–707
- Nève V, De La Roque ED, Leclerc F, Leteurtre S, Dorkenoo A, Sadik A, Cremer R, Logier R (2000) Ventilator-induced overdistension in children: dynamic versus low-flow inflation volume-pressure curves. *Am J Respir Crit Care Med* 162:139–147
- Gama de Abreu M, Heintz M, Heller A, Szechenyi R, Albrecht DM, Koch T (2003) One-lung ventilation with high tidal volumes and zero positive end-expiratory pressure is injurious in the isolated rabbit lung model. *Anesth Analg* 96:220–228
- Carvalho AR, Jandre FC, Pino AV, Bozza FA, Saluh JI, Rodrigues R, Soares JH, Giannella-Neto A (2006) Effects of descending positive end-expiratory pressure on lung mechanics and aeration in healthy anaesthetized piglets. *Crit Care* 10:R122

10. Carvalho AR, Jandre FC, Pino AV, Bozza FA, Salluh JI, Rodrigues R, Ascoli FO, Giannella-Neto A (2007) Positive end-expiratory pressure at minimal respiratory elastance corresponds to the best compromise between mechanical stress and lung aeration in oleic acid-induced lung injury. *Crit Care* 11:R86
11. Suarez-Sipmann F, Bohm SH, Tusman G, Pesch T, Thamm O, Reissmann H, Reske A, Magnusson A, Hedenstierna G (2006) Use of dynamic compliance for open lung positive end-expiratory pressure titration in an experimental study. *Crit Care Med* 35:214–221
12. Lachmann B, Robertson B, Vogel J (1980) In vivo lung lavage as an experimental model of the respiratory distress syndrome. *Acta Anaesthesiol Scand* 24:231–236
13. Uhl RR, Lewis FJ (1974) Digital computer calculation of human pulmonary mechanics using a least squares fit technique. *Comput Biomed Res* 7:489–495
14. Malboisson LM, Muller JC, Constantin JM, Lu Qin, Puybasset L, Rouby JJ, The CT Scan ARDS Study Group (2001) Computed tomography assessment of positive end-expiratory pressure-induced alveolar recruitment in patients with acute respiratory distress syndrome. *Am J Respir Crit Care Med* 163:1444–1450
15. Crotti S, Mascheroni D, Caironi P, Pelosi P, Ronzoni G, Mondino M, Marini JJ, Gattinoni L (2001) Recruitment and derecruitment during acute respiratory failure: a clinical study. *Am J Respir Crit Care Med* 164:131–140
16. Luecke T, Meinhardt JP, Herrmann P, Weiss A, Quintel M, Pelosi P (2006) Oleic acid vs saline solution lung lavage-induced acute lung injury: effects on lung morphology, pressure-volume relationships, and response to positive end-expiratory pressure. *Chest* 130:392–401
17. Musch G, Bellani G, Vidal Melo MF, Harris RS, Winkler T, Schroeder T, Venegas JG (2007) Relation between shunt, aeration and perfusion in experimental acute lung injury. *Am J Respir Crit Care Med* 177:292–300
18. Hedenstierna G (2003) Alveolar collapse and closure of airways: regular effects of anaesthesia. *Clin Physiol Funct Imaging* 23:123–129
19. Pelosi P, Rocco PR (2007) Airway closure: the silent killer of peripheral airways. *Crit Care* 11:114
20. Pelosi P, D'Andrea L, Vitale G, Pesenti A, Gattinoni L (1994) Vertical gradient of regional lung inflation in adult respiratory distress syndrome. *Am J Respir Crit Care Med* 149:8–13
21. Puybasset L, Gusman P, Muller JC, Cluzel P, Coriat P, Rouby JJ (2000) Regional distribution of gas and tissue in acute respiratory distress syndrome. III. Consequences for the effects of positive end-expiratory pressure. *CT Scan ARDS Study Group. Intensive Care Med* 26:1215–1227
22. Vieira SR, Puybasset L, Richecoeur J, Lu Q, Cluzel P, Gusman PB, Coriat P, Rouby JJ (1998) A lung computed tomographic assessment of positive end-expiratory pressure-induced lung overdistension. *Am J Respir Crit Care Med* 158:1571–1577
23. Rouby JJ, Puybasset L, Nieszkowska A, Lu Q (2003) Acute respiratory distress syndrome: lessons from computed tomography of the whole lung. *Crit Care Med* 31:S285–S295
24. Rouby JJ, Lu Q, Vieira S (2003) Pressure/volume curves and lung computed tomography in acute respiratory distress syndrome. *Eur Respir J* 22:27S–36S
25. Rouby JJ (2003) Lung overinflation. The hidden face of alveolar recruitment. *Anesthesiology* 99:2–4
26. Grasso S, Terragni P, Mascia L, Fanelli V, Quintel M, Herrmann P, Hedenstierna G, Slutsky AS, Ranieri VM (2004) Airway pressure-time curve profile (stress index) detects tidal recruitment/hyperinflation in experimental acute lung injury. *Crit Care Med* 32:1018–1027
27. Terragni PP, Rosboch GL, Lisi A, Viale AG, Ranieri VM (2003) How respiratory system mechanics may help in minimising ventilator-induced lung injury in ARDS patients. *Eur Respir J* 22:15S–21S
28. Nieszkowska A, Lu Q, Vieira S, Elman M, Fetita C, Rouby J-J (2004) Incidence and regional distribution of lung overinflation during mechanical ventilation with positive end-expiratory pressure. *Crit Care Med* 32:1496–1503
29. Puybasset L, Cluzel P, Gusman P, Grenier P, Preteux F, Rouby JJ (2000) Regional distribution of gas and tissue in acute respiratory distress syndrome. I. Consequences for lung morphology. *CT Scan ARDS Study Group. Intensive Care Med* 26:857–869
30. Rouby JJ, Puybasset L, Cluzel P, Richecoeur J, Lu Q, Grenier P (2000) Regional distribution of gas and tissue in acute respiratory distress syndrome. II. Physiological correlations and definition of an ARDS Severity Score. *CT Scan ARDS Study Group. Intensive Care Med* 26:1046–1056
31. Gattinoni L, Caironi P, Cressoni M, Chiumello D, Ranieri VM, Quintel M, Russo S, Patroniti N, Cornejo R, Bugedo G (2006) Lung recruitment in patients with the acute respiratory distress syndrome. *N Engl J Med* 354:1775–1786
32. Gattinoni L, Caironi P, Pelosi P, Goodman LR (2001) What has computed tomography taught us about the acute respiratory distress syndrome? *Am J Respir Crit Care Med* 164:1701–1711
33. Pelosi P, Cereda M, Foti G, Giacomini M, Pesenti A (1995) Alterations of lung and chest wall mechanics in patients with acute lung injury: effects of positive end-expiratory pressure. *Am J Respir Crit Care Med* 152:531–537
34. Neumann P, Berglund JE, Mondéjar EF, Magnusson A, Hedenstierna G (1998) Dynamics of lung collapse and recruitment during prolonged breathing in porcine lung injury. *J Appl Physiol* 85:1533–1543